Numerical Simulation of the Spin-Draw Process of Poly(ethylene terephthalate) Fibers

Tae Hwan Oh

Huvis R&D Center, 1690-1, Shinil Dong, Daedeok Ku, Daejeon, South Korea

Received 12 July 2006; accepted 19 October 2006
DOI 10.1002/app.25882
Published online in Wiley InterScience (www.interscience.wiley.com).

ABSTRACT: Numerical simulation for the calculation of the profile developments of the spin-draw process in the melt spinning of poly(ethylene terephthalate) was performed. Both spinning and drawing profiles were analyzed and included the structure development of birefringence and crystallinity in the draw line. By applying a simple model describing the continuous drawing process, we made it possible to simulate the spin-draw process. The strain rate of the spinline had a broad distribution, and that of the draw line had a narrower peak. The calculated birefringence ranged from 0.176 to 0.192 and the crystallinity ranged from 0.37 to 0.44 with draw ratio. The birefringence profile had a similar pattern as the stress profile, and the crystallinity gently increased along the draw line more than the birefringence did. © 2007 Wiley Periodicals, Inc. J Appl Polym Sci 104: 2522–2527, 2007

Key words: spin-draw process; profiles developments; numerical simulation

INTRODUCTION

The drawing process is essential to obtain desired final properties of textile products, and it has been performed in series or separate operations after spinning. It is a continuous deformation process accompanying the dimensional and physical property changes. Drawing has similar characteristic as spinning in terms of elongational deformation, but the former is the deformation in the solid state, and the latter is performed in the molten state. Also, it shows different behavior in the transfer of thermal energy. In melt spinning, the melt extruded from a spinneret flows down and contacts an atmosphere of quenched air, which is needed for solidification; however, in the drawing process, solidified material is heated to be deformable in a hot liquid or on a hot roller.

Many authors have carried out studies on melt spinning, and there have been great developments in the numerical simulation analyzing the dynamics of the melt-spinning process. [1–3] The drawing process, however, has been analyzed mainly by experiment. The effect of drawing conditions on the molecular structure and physical properties[4,5] and the drawing method[6–11] for an attainable maximum stretching of polymers have been studied. For example, the microwave heat-drawing technique,[6,7] zone drawing,[8,9] and ultradrawing with ultra-high-molecular-weight polyethylene[10,11] have been studied to improve mechanical properties. Also, structural modeling explaining the morphologies of drawn polymers has been investigated.[12] Drawing is a nonlinear deformation process, and the dynamics of the drawing process is similar to that of spinning in mass and momentum transfers. The differences between the drawing and spinning processes lie in the constitutive equation.[13,14] The spin-draw process has been become a typical manufacturing method of melt-spun synthetic fibers, but there has still been a lack of study of the dynamics of the spin-draw process. Only the simulation of the spinning and drawing processes have been of focus.

In this study, we examined the simulation of the spin-draw process. The dynamics of the spin-draw process was analyzed, and the profile developments along the spinning and drawing line were simulated.

FORMULATION AND NUMERICAL METHOD

A cylindrical coordinate system was used for this numerical procedure. For steady, incompressible melt flow in the spinning, the asymptotic equations averaged over a cross-section for conservation of mass, momentum, and energy are as follows:

$$W = \rho A v_z \tag{1}$$

$$dF/dz = W(dv_z/dz - g/v_z) + \pi\rho_a v_z^2 C_f D/2 \tag{2}$$

$$dT/dz = -\pi D h(T - T_a)/(WC_p) \tag{3}$$

where W is the mass flow rate of the polymer, ρ is the density, A is the area of the fiber, v_z is the axial

Correspondence to: T. H. Oh (ohth@huvis.com).

Journal of Applied Polymer Science, Vol. 104, 2522–2527 (2007)

TABLE I
Material Parameters Used in the Simulation

Parameter	Value
k_a (g·cm/s^3·°C)	2.63×10^3
μ_a (cm^2/s)	0.29
C_p of PET (cm^2/s^2·°C)	$(0.3+6.0 \times 10^{-4}T) \times 4.2 \times 10^7$
Density of PET (g/cm^3)	$1.356–5 \times 10^{-4}T$

velocity, ρ_a is the density of air, F is the force, z is the position in the axial direction, D is the diameter, C_f is the skin friction coefficient, g is the gravity constant, C_p is the specific heat capacity of the polymer, h is the heat transfer coefficient of the polymer, T is the temperature of the polymer, and T_a is the temperature of the surrounding air. Here, Newtonian fluid as constitutive equations of melt spinning was assumed. The constitutive equation of fluid is presented as

$$F = \eta A(dv_z/dz) \tag{4}$$

where η is the elongational viscosity.

η of poly(ethylene terephthalate) (PET) was assumed to be only a function of temperature and expressed as follows:[15]

$$\eta = 0.73 \times \exp\left(\frac{5300}{T+273}\right) \tag{5}$$

To derive the previous equations, a purely extensional flow field was assumed, and the viscous dissipation was neglected. The basic equations were strongly coupled with a lack of one more single equation for analytical calculation. Therefore, a shooting method was used with an initial guess of F at the die (at $z = 0$) to fit the boundary condition of spinning speed. The boundary conditions applied in the simulation are expressed as:

$$T(0) = T_{\text{die}}, \quad v_z(0) = v_0, \quad v_z(v) = v \tag{6}$$

where T_{die} is the spinning temperature, v_0 is the initial speed, v_1 is the velocity of the first godet roller, and L_1 is the distance from the spinneret to the first godet roller. The dimension of the spinneret as the starting D in the simulation was used. Because the spinning process had a large length-to-D ratio, the die swell effect could be neglected.[16] Several correlations for the physical properties and transport coefficients are expressed as follows, and some material parameters are summarized in Table I:[15–20]

$$h = 0.42\left(\frac{k_a}{D}\right)\text{Re}_d^{0.334}\left[1+\left(\frac{8v_a}{v_z}\right)^2\right]^{0.1667} \tag{7}$$

$$C_f = 0.37\text{Re}_d^{-0.61} \tag{8}$$

$$\text{Re}_d = \left(\frac{v_z D}{\mu_a}\right) \tag{9}$$

where k_a is the thermal conductivity of air, v_a is the quench air velocity, μ_a is the kinematic viscosity of air, and Re_d is the Reynolds number.

The plug and extensional flow field and isothermal conditions were assumed to simulate a drawing process. A constant drawing F along the draw line, the incompressibility of the fiber, and a steady state were assumed:

$$F = \sigma A = \text{Constant.} \tag{10}$$

$$\sigma = \frac{F}{A} = \frac{\rho F}{W}v_z \tag{11}$$

where σ is the true stress. The constitutive equation describing the drawing process of solid polymer was introduced as[13,21]

$$\sigma = k[1-\exp(-\omega\varepsilon)]\exp(h\varepsilon^2)(\dot{\varepsilon}/\dot{\varepsilon}_0)^m \tag{12}$$

where ε is the true strain, $\dot{\varepsilon}$ is the true strain rate of the filament at distance z, and $\dot{\varepsilon}_0$ is the reference strain rate (conventionally equal to 1 s^{-1}). k, ω, h, and m are the rheological parameters representing the scaling factor, strain hardening factor, viscoelastic coefficient, and strain rate sensitivity coefficient, respectively.[13,14] This equation was used as a constitutive equation describing the stretching behav-

TABLE II
Conditions of the Spin-Draw Process in the Simulation

No.	W (g min^{-1}·hole^{-1})	T_{die} (°C)	First godet roller speed (m/min)	v_a (m/s)	Quench air temperature (°C)	Second godet roller speed (m/min)
1	1.04	290	1000	0.3	25	4500
2	1.04	290	1125	0.3	25	4500
3	1.04	290	1285.7	0.3	25	4500
4	1.04	290	1500	0.3	25	4500

TABLE III
Rheological Parameters of PET Used in the Drawing Simulation

k(Mpa)	ω	h	m
17	15	0.55	0.06

ior of semicrystalline polymers and was used to describe the uniaxial fiber drawing. The boundary conditions for drawing are expressed as

$$v_z(L_1) = v_1, \quad v_z(L_2) = v_2 \tag{13}$$

where v_2 is the velocity of the second godet roller and L_2 is the length of yarn path between spinner and second godet roller. In a steady-state continuous drawing process, the local ε and $\dot{\varepsilon}$ can be expressed as

$$\varepsilon = \ln\left(\frac{l}{l_0}\right) = \ln\left(\frac{v}{v_1}\right) \tag{14}$$

$$\dot{\varepsilon} = \frac{d\varepsilon}{dt} = \frac{d\varepsilon}{dz}\frac{dz}{dt} = v\frac{d\varepsilon}{dz} \tag{15}$$

where l is the current length of the filament element and l_0 is its initial value. The relation between z and ε is expressed as[13,14]

$$z = \frac{v_1}{\dot{\varepsilon}}\left(\frac{k}{\sigma_0}\right)^{1/m}\int_0^{\varepsilon} R(\varepsilon)d\varepsilon \tag{16}$$

$$R(\varepsilon) = \exp(\varepsilon)\left[\exp(h\varepsilon^2 - \varepsilon) - \exp(h\varepsilon^2 - (\omega+1)\varepsilon\right]^{1/m} \tag{17}$$

During the drawing stage, the orientation-induced crystallization takes place, and a final molecular structure is formed. Nakamura et al.[22] proposed a modified Avrami equation, and the relation is expressed as

$$\frac{dX_c}{dz} = \frac{KX_\infty}{v}\left(1 - \frac{X_c}{X_\infty}\right) \tag{18}$$

where X_c is the crystallinity, K is the crystallization rate parameter, and X_∞ is the limiting crystallinity. Katayama and Yoon[23] proposed an equation for the crystallization parameter of PET, and it was used in the simulation:

$$\frac{K}{K_0} = \exp\left[\frac{1.2\times10^6}{(T+273)\Delta T}\left(1 - \frac{1}{1+160(T+273)\Delta n^2/\Delta T}\right)\right] \tag{19}$$

$$K_0 = \exp\left[9.34 - \frac{682}{T-43} - \frac{4.53\times10^5}{(T+273)\Delta T}\right] \tag{20}$$

$$\Delta n = 0.2\left[1 - \exp\left(-\frac{1.65\times10^{-6}\sigma}{T+273}\right)\right] \tag{21}$$

where ΔT and Δn are the supercooling and the birefringence, respectively, and K_0 is the crystallization rate constant. The initial D of spinneret in the simulation was 0.3 mm.

The fourth-order Runge–Kutta method was used to solve the asymptotic equation describing the dynamics of melt spinning, and a Romberg algorithm was used to solve eq. (16). The conditions of the spin-draw process and the rheological parameters are presented in Tables II and III, respectively.

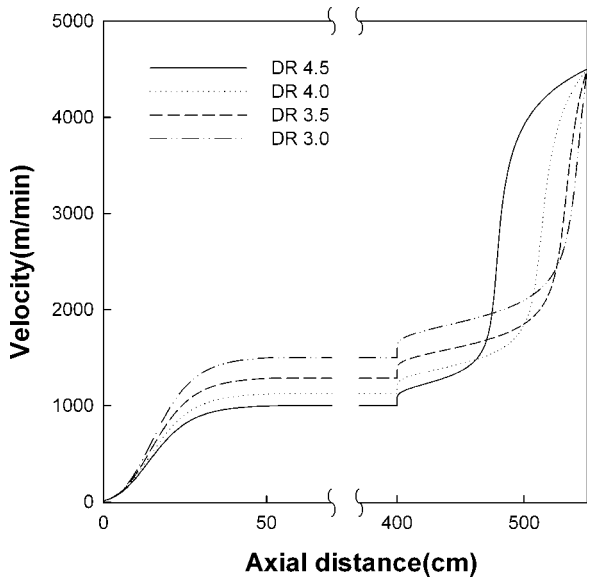

Figure 1 Velocity profiles in the spin-draw process along the axial distance. DR, draw ratio.

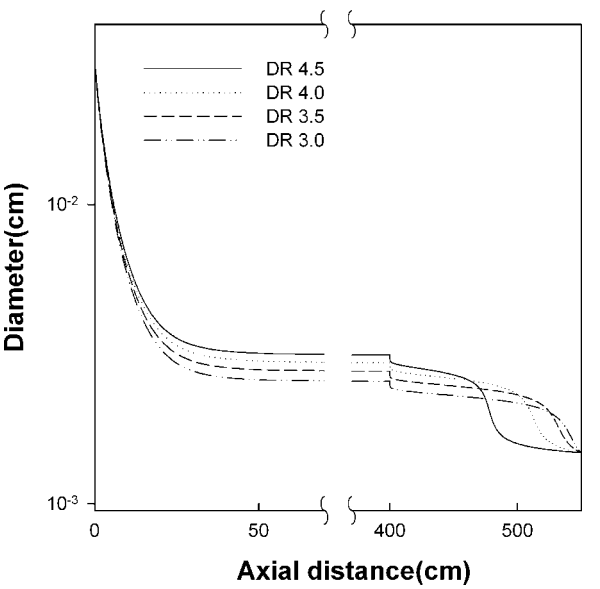

Figure 2 D profiles in the spin-draw process along the axial distance. DR, draw ratio.

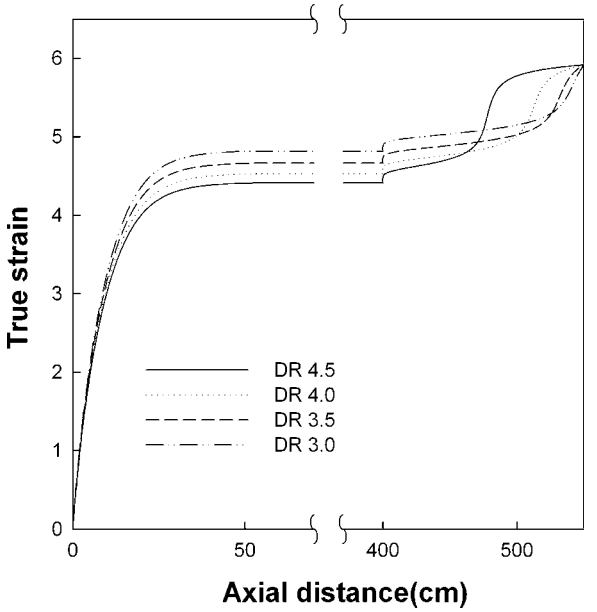

Figure 3 ε profiles in the spin-draw process along the axial distance. DR, draw ratio.

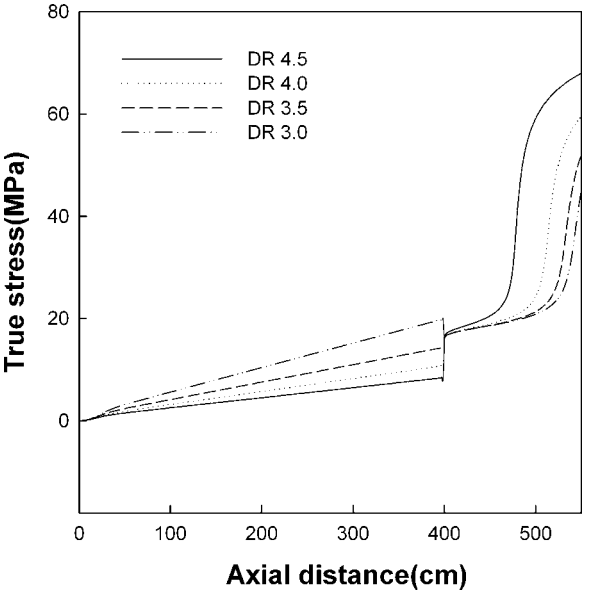

Figure 5 σ profiles in the spin-draw process along the axial distance. DR, draw ratio.

RESULTS AND DISCUSSION

The spin-draw process in melt spinning is composed of a spinning zone, a drawing zone, and a take-up zone. The extrudate from the spinneret stretches and solidifies between the spinneret and the first godet roller, and then, as-spun filaments are drawn between the two godet rollers. In this study, a numerical simulation was executed in the spinning and drawing zones because there was no profile development in the take-up zone. By heat drawing, the filament achieves its final dimension and physical properties. Velocity, temperature, *D*, and *F* profiles were developed along the spinning and drawing line. Figure 1 shows the velocity buildup in the spin-draw process for different draw ratios at the same take-up speed. The velocity profiles of the running filament in the spinline and draw line were a form of sigmoid, but a slight difference was observed. The fiber elements were accelerated from their initial to final

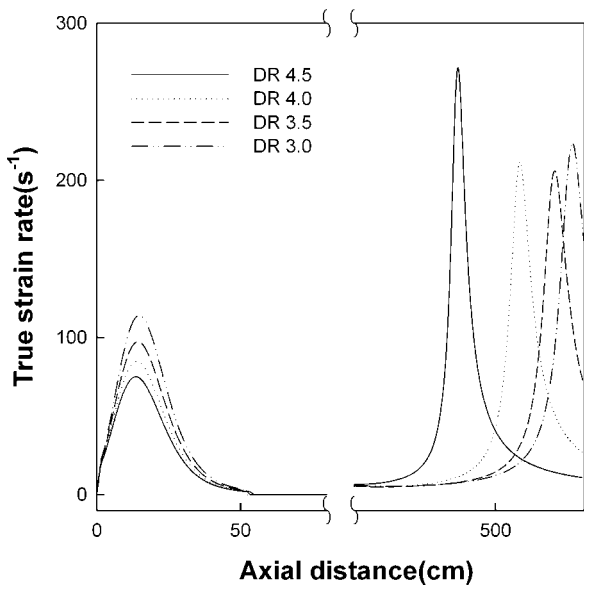

Figure 4 True strain rate profiles in the spin-draw process along the axial distance. DR, draw ratio.

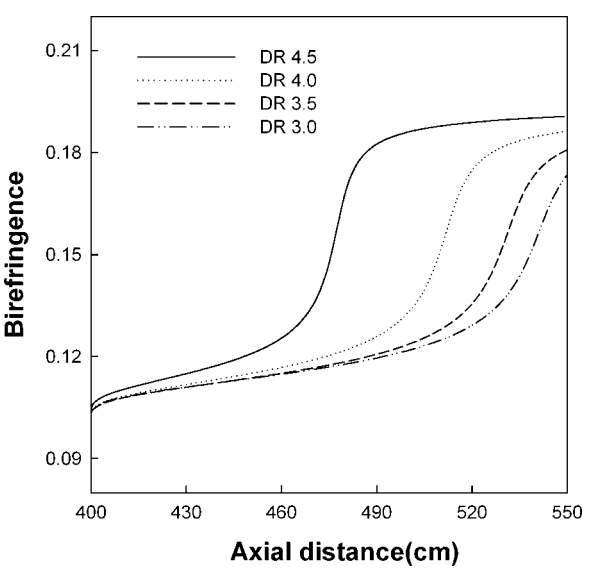

Figure 6 Δn profiles in the spin-draw process along the draw line. DR, draw ratio.

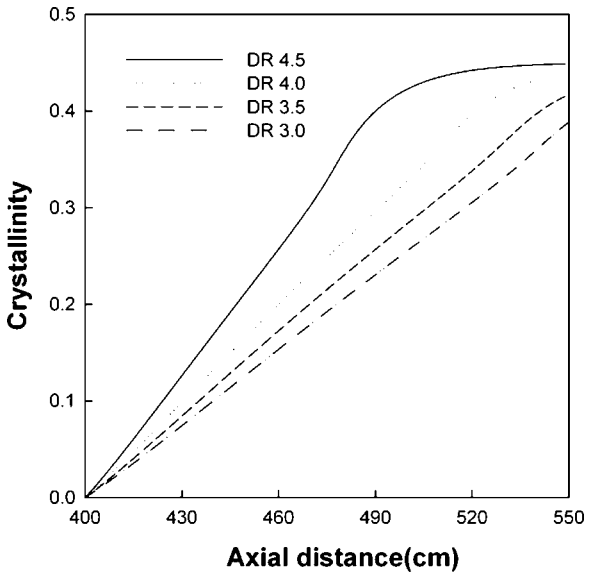

Figure 7 X_c profiles in the spin-draw process along the draw line. DR, draw ratio.

velocity. Here, the final velocity was the first godet roller speed for the spinning zone and the second godet roller speed for the drawing zone. The velocity buildup in the spinline showed a smooth increase from the spinneret to a solidification point along the axial distance, but the velocity in the draw line increased steeply at the deformation concentration region. The simulated D profile along the axial distance is shown in Figure 2. D decreased exponentially in the spinline, but an abrupt decrease at certain point occurred (Fig. 2) because of strain localization in the draw line. As shown in Figure 1, the smooth velocity increase in the spinline led to a gentle decrease in D. On the other hand, a steep increase in the velocity in the draw line led to an abrupt decrease in the D profile. Figure 3 shows ε profiles. Like the separate low-speed continuous drawing,[13,14] similar deformation kinetics, such as strain hardening and strain localization, were observed in the drawing line of the spin-draw process. There was difference between ε of the spinning zone and that of drawing zone. Unlike the strain profile of the spinning zone, that of the drawing zone had a sigmoidal shape with an inflexion point and a horizontal asymptote at the end of deformation zone. The inflexion point moved toward the first godet roller with increasing draw ratio. Figure 4 shows the ε rate profile along the axial distance. The strain rate had its maxima in both the spinning and drawing lines, but their shapes and magnitudes were different. The strain rate of the spinline had a broad distribution, and its maximum value was between 74.9 and 112.2 s^{-1}, but that of the draw line had a narrower peak and ranged from 206.1 to 271.7 s^{-1}. Because of strain localization in the draw line, the strain rate in the draw line was greater than that in the spinline. z of the maximum peak moved near the first godet with increasing draw ratio. Figure 5 shows σ profiles. The σ profile in the spinline decreased with draw ratio. This was because v_1 increased with decreasing draw ratio. From the F balance of the spinline [eq. (2)], F acting on the spinline increased with velocity buildup. However, in the draw line, σ was proportional to ε and the true strain rate, that is, the draw ratio.

The analysis for structure development of the orientation and the crystallization kinetics is important for explaining the drawing process of crystalline polymers. Figures 6 and 7 show Δn and X_c profiles along the draw line. Δn revealed a similar pattern as σ, and its values ranged from 0.176 to 0.192 with draw ratio. X_c ranged from 0.37 to 0.44. The X_c profiles of the spin-draw process showed different patterns in comparison with those of high-speed spinning. In high-speed spinning, there is an abrupt increase in X_c when the crystallization takes place,[15] but in this study, X_c in the draw line increased steadily along the axial distance. In high-speed spinning, an abrupt increase in X_c takes places because of stress-induced crystallization, and Δn increases. However, X_c in the draw line of the spin-draw process gently increased more than Δn did.

CONCLUSIONS

The spin-draw process of PET filaments, including the molecular orientation and crystallization dynamics, was analyzed with different constitutive equations for the spinning and drawing processes, respectively. The strain rate of the spinline had a broad distribution, and that of the draw line had a narrower peak. It ranged from 74.9 to 113.9 s^{-1} for the spinline and 206.1 to 271.7 s^{-1} for the draw line with draw ratio. The calculated Δn ranged from 0.176 to 0.192, and X_c ranged from 0.37 to 0.44. The Δn profile had a similar pattern as the stress profile, and X_c gently increased along the draw line more than Δn did.

References

1. Denton, J. S.; Cuculo, J. A.; Tucker, P. A. J Appl Polym Sci 1995, 57, 939.
2. Cao, J.; Kikutani, T.; Takaku, A.; Shimizu, J. J Appl Polym Sci 1989, 37, 2683.
3. Goerge, H. H. Polym Eng Sci 1982, 22, 292.
4. Baht, K. K.; Bell. J. P. J Polym Sci 1990, 39, 319.
5. Mocherla, N. V.; Naik. S. G. J Polym Sci 1984, 54, 868.
6. Suzuki, A.; Mochiduki, N. J Appl Polym Sci 2001, 82, 2775.
7. Suzuki, A.; Ishihara, M. J Appl Polym Sci 2002, 83, 1711.
8. Kunugi, T.; Suzuki, A.; Hashimoto, M. J Appl Polym Sci 1981, 26, 1951.

9. Kunugi, T.; Suzuki, A.; Hashimoto, M.; Matsusaki, K. Polymer 1981, 23, 1983.
10. Smith, P.; Chanzy, H. D.; Rotzinger, B. P. J Mater Sci 1987, 22, 523.
11. Gerrits, N. S. J. A.; Tervoort, Y. J Mater Sci 1992, 27, 1385.
12. Peterlin, A. J Mater Sci 1971, 6, 490.
13. Lee, M. S.; Oh, T. H.; Kim, S. Y.; Shim, H. J. J Appl Polym Sci 1999, 74, 1836.
14. Lee, M. S.; Kim, S. Y. J Appl Polym Sci 2001, 81, 2170.
15. Shimizu, J.; Okui, N.; Kikutani, T. High-Speed Fiber Spinning; Wiley-Interscience: New York, 1985; p 173.
16. Oh, T. H. Polym Eng Sci 2006, 46, 609.
17. George, H. H.; Holt, A.; Buckley, A. Polym Eng Sci 1980, 23, 95.
18. Dutta, A.; Nadkarni, V. M. Text Res J 1984, 54, 778.
19. Matsuo, T. J Appl Polym Sci 1976, 20, 367.
20. Dutta, A.; Nadkarni, V. M. Text Res J 1984, 54, 35.
21. G'Sell, C.; Marquez-Lucero, A. Polymer 1993, 34, 2740.
22. Nakamura, K.; Katayama, K.; Amano. T. J Appl Polym Sci 1993, 17, 1031.
23. Katayama, K.; Yoon, M. G. High-Speed Fiber Spinning; Wiley-Interscience: New York, 1985; p 207.